TRIDIMENSIONAL NUMERICAL SIMULATION OF AIR CURRENTS IN AN INDUSTRIAL BREAD TUNNEL PROVER

Adriana ISTUDOR[1], Gheorghe VOICU[2], Gheorghe MUSCALU[3]

Industrial provers are air conditioned, temperature and relative humidity being two parameters of interest. Equally important is the air speed distribution in the prover, which is performed with a set of tubes specifically placed for treated air recirculation. The purpose of this paper is the analysis and determination of optimal air speed distribution in a 4 level tunnel prover for uniform temperature distribution throughout the entire prover volume.

Keywords: bread dough prover; air distribution speed; numerical 3D simulation; air distribution pipes.

1. Introduction

In bread making, the proving process is a defining stage which establishes crumb structure and overall appearance of the bread piece, [1, 2]. The proving process of dough takes place in enclosed spaces called provers, [3]. The modern models have air conditioning systems with hot or cold heat exchangers, steam supply, fan and air filters; the air distribution in the prover is done using charge and discharge air pipe lines, [4, 5, 6, 7]. The air conditioning system must be dimensioned for ensuring the necessary working parameters: temperature and relative humidity. One of the most important aspects is that the conditioned air must be related with the speed of air inlet so as to ensure a uniform air distribution inside the prover but also to limit humidity losses from the loaves to the environment, which results in crust formation on the surface of the loaf and affects the product quality, [1]. In some situations, for pressure loss compensation in the distribution pipes, different dimension solutions are used. There is also the possibility to use different dimensions for the ventilation openings. Ventilation effectiveness can be evaluated by either measurement or simulation, [9]. In simple terms, the ventilation flow rate can be measured by measuring how quickly injected tracer gas is decayed in a room, or by measuring the air velocity through ventilation openings or air ducts, as well as the flow area. The airflow direction may be visualized by smoke.

[1] PhD student, Faculty of Biotechnical Systems Engineering, University POLITEHNICA of Bucharest, email: istudor.adriana@mgbiotech.ro
[2] Prof., Faculty of Biotechnical Systems Engineering, University POLITEHNICA of Bucharest, email: ghvoicu_2005@yahoo.com
[3] PhD eng. Company MG BIOTECH SRL, Bucharest, email: gheorghe.muscalu@mgbiotech.ro

Computational fluid dynamics and particle image velocimetry techniques allow the air distribution performance in a room to be modelled (CFD), [9, 10, 11, 12, 13, 14]. In food industry, CFD has been successfully applied to processes such as drying, refrigeration, cooling, sterilization, pasteurization, [15]. In bread making, CFD applications are found for the studying of dough kneading and mixers design, [16, 17, 18] and bread baking, regarding aspects like heat flow and distribution of air, speed and pressure in the oven, [19, 20, 21]. Even though proving is a key stage in bread making with considerable influence on the finished product, no CFD applications can be found in literature. Worldwide bread making equipment manufacturers have lately expressed an interest in computer designing flow patterns in provers and acknowledged the necessity for better control of the proving regime, [22].

The purpose of this paper is the analysis and determination of optimal recirculated air speed in regard to a uniform dispersion of temperature through the entire volume of the prover and without negatively affectation of dough rheological characteristics.

In the first part of the paper, it was performed a tridimensional simulation at reduced scale prover (one floor with two rows of dough pieces) in which it was analyzed the degree of uniformity for temperature parameter at different air speeds: 0.2 m/s, 0.4 m/s and 0.6 m/s. The best results were obtained at the air speed of 0.6 m/s.

In the second part of the paper the tridimensional simulation was performed for real scale prover where the geometry of the discharge grids and air flow were modified to obtain an air speed of 0.6 m/s on all the prover's floors. The best results were obtained at a vent frequency of 50 Hz and the established dimensions of the grids as follows (from top to bottom):A=400 x 200 (mm), B=400 x 200 (mm), C=300 x 180 (mm), D=250 x 150 (mm), E= 200 x 100 (mm).

With this kind of simulation it can be determined the optimal air speed which allows a good temperature uniformity in the entire space of the prover without negatively influencing the superficial layers of the dough pieces (e.g. excessive humidity loss).

2. Materials and methods

The computational program for tridimensional simulation, Ansys Fluent is used in a two part simulation of air current flow during dough proving. In the first part of the simulation the tridimensional model is applied to one floor of the prover. In the second part of the simulation, the model is applied to prover's real scale, using the values determined in the first part.

The stages for tridimensional analysis can be observed in figure 1.

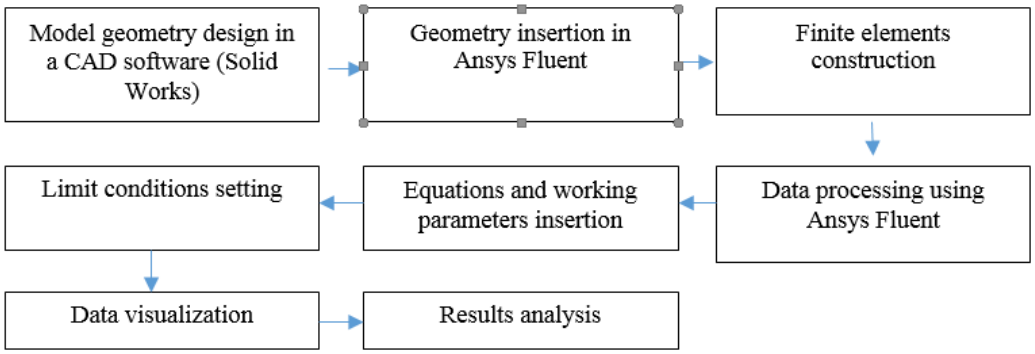

Fig 1. Stages for performing the tridimensional simulation in Ansys

The mathematical model used for this tridimensional model, which is integrated in the Ansys Fluent package, uses the energy equation, [23].

Ansys Fluent solves the energy equation in the following form:

$$\frac{\partial}{\partial_t}(\rho E) + \nabla\left(\vec{v}(\rho E + \rho)\right) = \nabla(k_{eff}\nabla T - \sum_j h_j \overrightarrow{Jj} + (\bar{\bar{\tau}}eff * \vec{v})) + S_h \qquad (1)$$

where: k_{eff} is the actual thermal conductivity ($k + k_t$ where k_t is turbulent thermal conductivity). The first three terms from the right part of equation describe the energy transfer through conduction, particle flow diffusion, $\overrightarrow{Jj}$ and viscous dissipation respectively. S_h includes the heat from the chemical reaction and any other defined volumetric sources.

The material enthalpy is determined as the sum of sensible enthalpy h and latent heat Δh:

$$H = h + \Delta h \qquad (2)$$

where:

$$h = h_{ref} + \int_{T_{ref}}^{T} c_p \, dT \qquad (3)$$

and: h_{ref} is the reference enthalpy, T_{ref} is the reference temperature, c_p is the specific evaporation heat at constant pressure.

The liquid friction β, is defined as: β = 0, if T< T_{solid}; β=1, if T> T_{liquid}; β= $\frac{T-T_{solid}}{T_{liquid}-T_{solid}}$, if $T_{solid} < T < T_{liquid}$.

The latent heat content can be written in terms of material latent heat, L. It results:$\Delta H = \beta_L$.

The latent heat content can vary between 0 for a solid and L for a liquid.

For solidification/melting problems, the energy equation is written as follows, [24, 25, 26, 27, 28]:

$$\frac{\partial}{\partial_t}(\rho H) + \nabla(\rho \vec{v} H) = \nabla(k \nabla T) + S \quad (4)$$

where: H = enthalpy, ρ=density, $\vec{v} = fluid\ speed$, S = term source, T-temperature (K).

The solution for temperature with which the Ansys software performs the calculations is in essence an iteration between the energy equation x and the liquid fraction y. Direct use of liquid fraction would result in a weak convergence for the energy equation. In Ansys fluent, the method used by Voller and Swaminathan is used to update the liquid fraction.

In the first simulation it was used the following data: one floor analysis with two rows of dough pieces with 360 g each, 17 dough pieces on each row, 60 mm distance (d) between each dough piece. The model is considered static. The proving floor has the following dimensions: L=3 m, l=0.6 m, h=0.31 m.

A series of hypotheses with which the model was run and generated were applied: the free interior space is full with air, the pressure is constant, p=101325 Pa, the air is introduced (effused) in the enclosed space through one side (left) and aspirated through the other side (right). The simulation was run at three air speeds: 0.2, 0.4 and 0.6 m/s respectively.

The working air temperature, which is diffused in the prover was established at T=318 K and other physical air properties: density, air specific heat constant (Cp), thermal conductivity, viscosity, which can be seen in figure 2.

The air volume (0.558 m^3) in the designed space was divided in a computational grid comprised in a triangular unstructured network with 50210 nodes, 218915 elements and 320005 facets.

In figure 3 is presented the designed floor in Solid Works in parallel with the real one, taken with permission in ALX-ROM factory, Rusanesti, Olt, Romania.

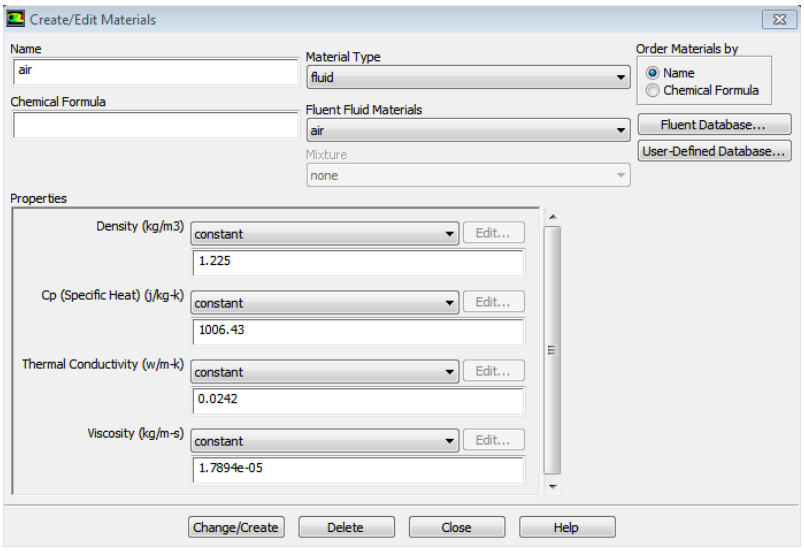

Fig. 2. Physical properties of air, inserted in Ansys Fluent software

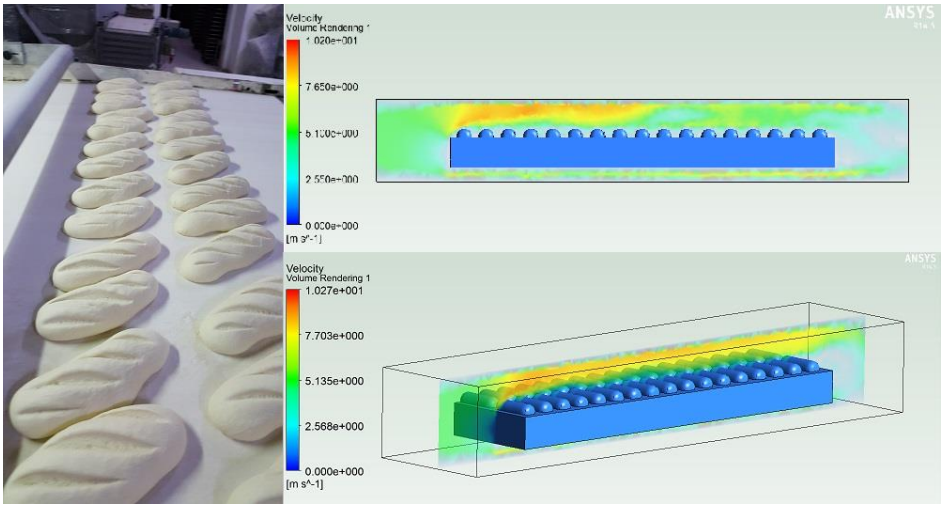

Fig. 3. Bread dough pieces: picture taken in ALX –ROM factory, Rusanesti, Olt, Romania (left) and the designed floor with dough pieces (right)

In the second simulation stage a real scale prover was designed, with the purpose of analyzing if a uniform distribution for air temperature can be achieved at 0.6 m/s on multiple prover floors.

The prover used for this simulation has 4 automated conveyors (figure 4). The conveyor which discharges the dough pieces at the oven entrance is loaded at the other end with fresh dough pieces, in which time, the other three conveyors are stationary. The process is consecutive and cyclic for each conveyor. The prover has the following dimensions: L=24m, l=3m, h=3m.

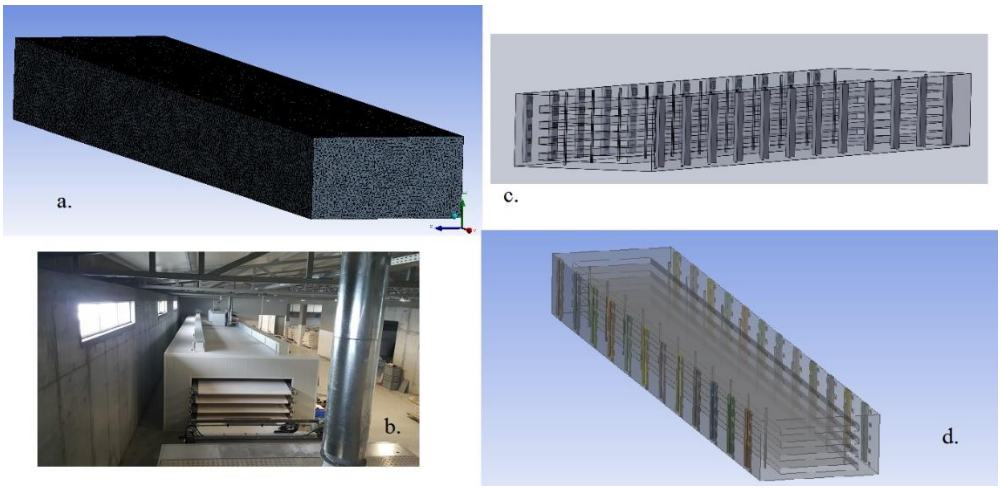

Fig. 4. Industrial dough prover: a-geometric model built using the finite element network; b. tunnel prover with 4 conveyors; c-designed model in Solid Works; d-the generated model in Ansys Fluent

The prover has an air conditioning system which uses a fan with a capacity of 2200 m³/h and an air distribution system, (figure 5).

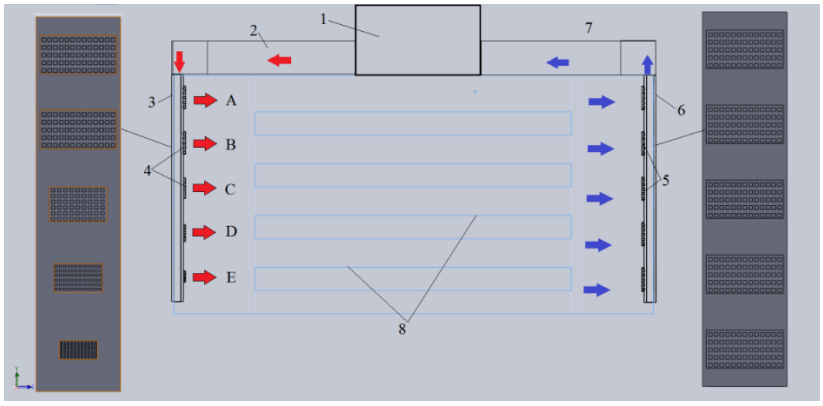

Fig. 5. The air distribution system design: 1-air conditioning system; 2-exterior pipes for air discharge; 3-interior pipes for air discharge; 4-air discharge grids; 5-air charge grids; 6-interior pipes for air charge; 7-exterior pipes for air charge; 8-prover floors

The air is blown through one side of the prover and aspirated through the other side, after it passes (charged with temperature) through the floors of the prover. The exterior charge (2) and discharge (7) air pipes have 0.09 m² diameter and are connected to 12 internal discharge (3) and charge (6) air distributers placed on the entire prover length, from 2 to 2 meters. Each internal distributor has 5 grids (4, 5), one for each floor and one for the space between the ground floor and the base of the prover. There are no registered differences for air speed through the grids placed on the length of the prover.

The air volume (216 m^3) in the enclosed designed prover has been divided in a computational grid comprised in an unstructured triangular network with a nodes number of 5002101, 2128915 elements and 3520005 facets.

The following hypotheses with which the model was run and finally generated were applied: the entire free space in the enclosure is full with air at constant pressure, p=101325 Pa. The air is introduced in the prover using the left grids and aspirated through the right grids with an air speed individually defined for each grid (the air speed values were determined through real measurements performed in the prover and which are presented in table 1). The model is static and the discharge air temperature was set at T=318 K. The recirculated air properties were defined as in figure 2 and for calculations it was used the energy equation from the Ansys Fluent software.

Optimization tests were performed for air flow inside the prover using different discharge grid sections until good results were obtained (figure 6).

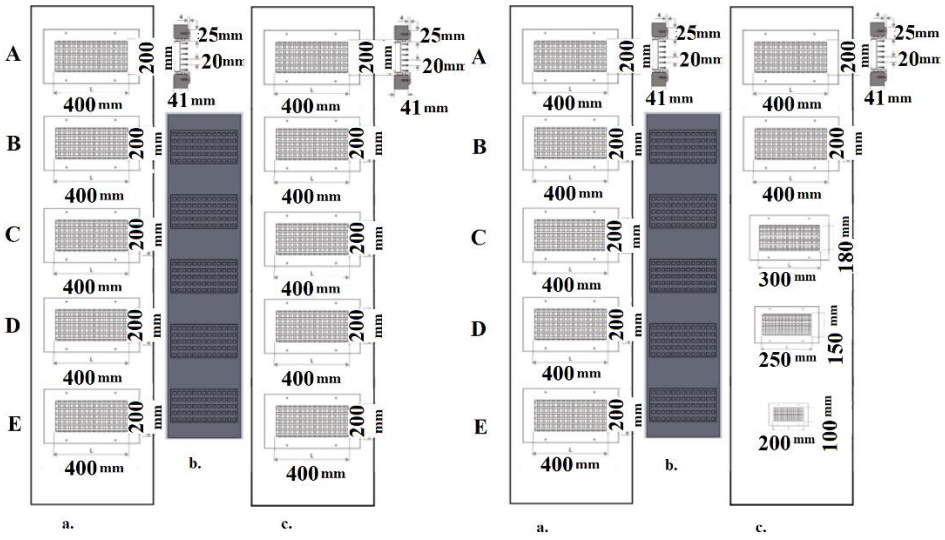

1. 2.

Fig. 6. 1.First case – a) Interior charge grids, b) Interior discharge grids designed in Solid Works, c) Interior discharge grids; 2. Second case – a). Interior charge grids, b) Interior discharge grids designed in Solid Works; c) Interior discharge grids

Starting from equal discharge grid sections, the dimensions were modified until the air speed and temperature implicitly were uniformly distributed on all prover floors.

In the first case, the discharge grids had the same dimensions: L=400mm and w=200mm. Simulations were performed for three air flow values. The air flow was modified through the variation of fan frequency. All the air charge grids had: L=400mm and w=200mm.

In the second case, the air discharge grids had the following dimensions (top to bottom): A- L=400mm and w=200mm; B-L=400mm and w=200mm; C-L=300mm and w=180mm; D- L=250mm and w=150mm, E- L=200mm and w=100mm. The air charge grids had equal dimensions: L=400mm and w=200mm. Simulations were performed for 4 different air flow values. The air flow was modified through the variation of fan frequency. There was also analyzed the influence of air flow change from 20 to 70 Hz, each 10 Hz interval.

3. Results and discussions

For the dough to be less affected by the air currents in the prover, it is very important to determine the minimal values at which the recirculated air ensures the temperature gradient required for the proving process and as uniformly dispersed as possible.

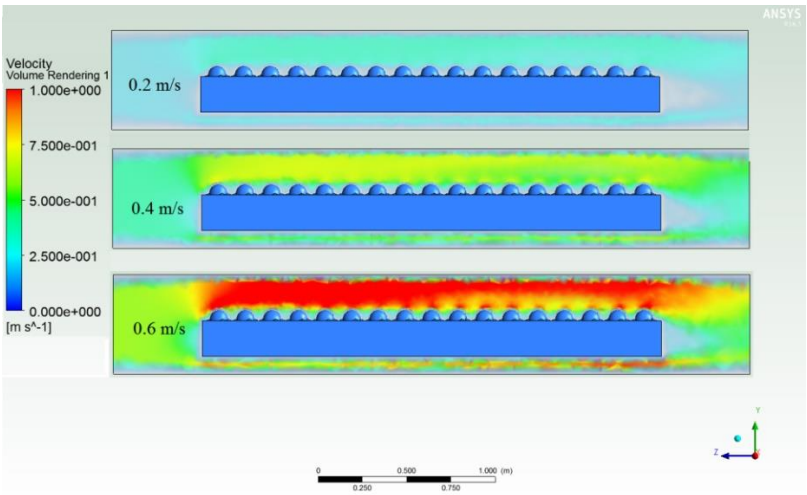

Fig. 7. Air speed distribution in the proving chamber based on the air speed

In figure 7 it can be observed that the air currents have a relatively constant speed at each analyzed air speed, but it is necessary to analyze in comparison the temperature distribution (figure 8) in order to establish which solution is the best.

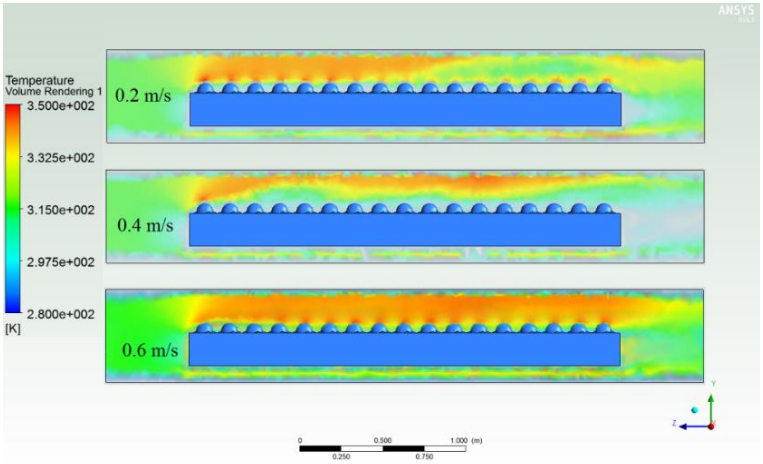

Fig. 8. Temperature distribution in the proving chamber based on air speed

Analyzing the temperature distribution at different air speeds, it can be observed that for values 0.2 m/s and 0.4 m/s, the temperature is not uniformly distributed. At 0.6 m/s, the temperature is much more uniformly distributed. From practice, it was observed that at higher air speed, the turbulent flow exceeds a critical point and it is necessary to compensate the humidity loss in order to maintain the physical characteristics of dough pieces.

The main purpose of the second tridimensional simulation was to achieve an air speed of 0.6 m/s through the entire prover. For this stage, the air discharge grids geometry and/or the air speed were modified. The air speed values entering the prover and used in the simulation are presented in table 1.

It is presented in figure 9, the air speed uniformity throughout the prover, using equal grid dimensions through the entire height of the prover. Because the air speed didn't reach 0.6 m/s, the fan frequency was modified from 50 Hz to 60 Hz and 70 Hz, respectively. Thus, the air flow changed from 2200 m³/h to 3950 m³/h.

Table 1

Values for air speed entering the prover through the grids, used in the simulation

Grid	**Equal grids**			**Different grids**			
	Fan frequency [Hz]						
	50	60	70	20	30	40	50
	Air speed [m/s]			**Air speed [m/s]**			
A	0.3	0.33	0.38	0.21	0.25	0.3	0.33
B	0.5	0.51	0.57	0.46	0.48	0.51	0.6
C	0.9	0.94	1.1	0.49	0.51	0.55	0.8
D	1.4	1.4	1.6	0.6	0.7	0.8	1
E	3	3.1	3.4	0.78	1.3	2	2.1

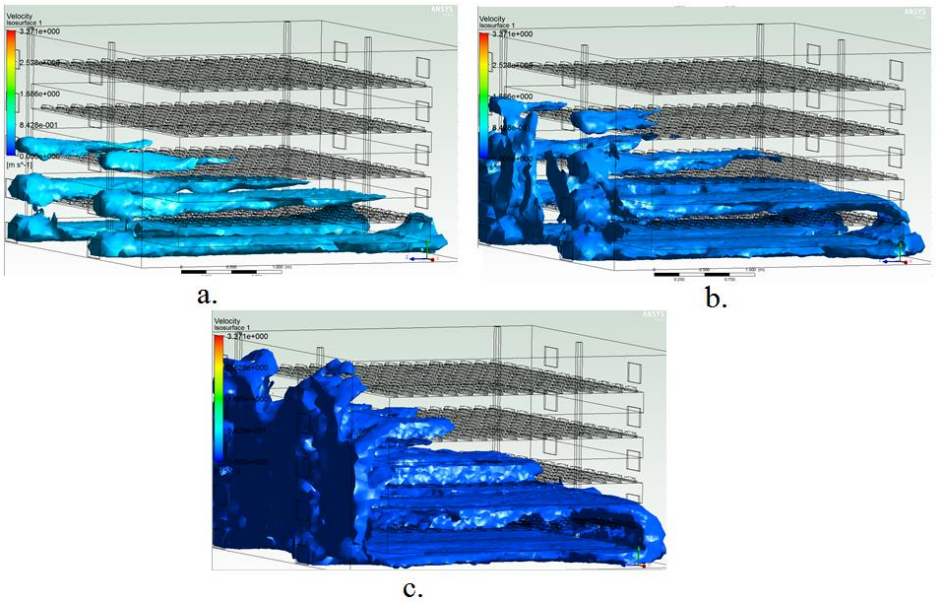

Fig. 9 Air speed distribution in the points where it reaches 0.6 m/s: a) fan working at 50 Hz simulation; b) fan working at 60 Hz simulation; c-fan working at 70 Hz simulation

At 50 Hz, the fan has an air flow of 2200 m³/h. In figure 9, the software analyzed which is the air distribution at 0.6 m/s. By increasing the air flow, the air currents are higher in the lower part of the prover (D and E grids). In grid E, the registered air speed has a value of 3.4 m/s and much lower on the superior grids. Analyzing this results, it seems necessary to dimension grids C, D and E in order to correctly distribute the air speed in the prover. Grid E has the main purpose to produce a thermal barrier between the ground and first floor. Also, in bread making industry, higher differences than +/-1 °C are not allowed between prover floors, because the products would register quality differences, mainly in volume and exterior characteristics.

In figures 10 and 11 is presented the comparative analysis between the simulations using equal discharge grid dimensions and modified grid dimensions.

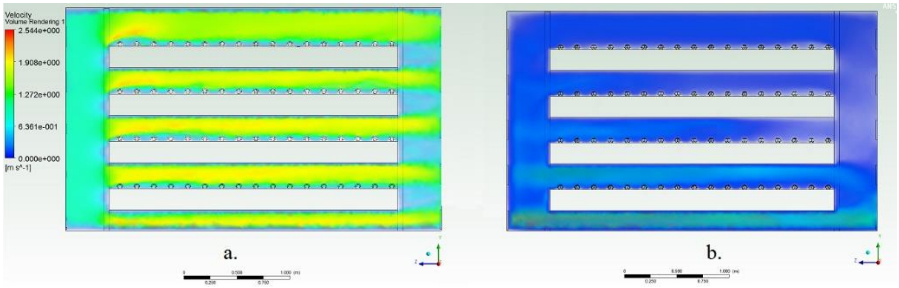

Fig. 10. Frontal view of the prover and air speed distribution at: a) different discharge grids, fan at 50 HZ; b) equal discharge grids, fan at 50 Hz

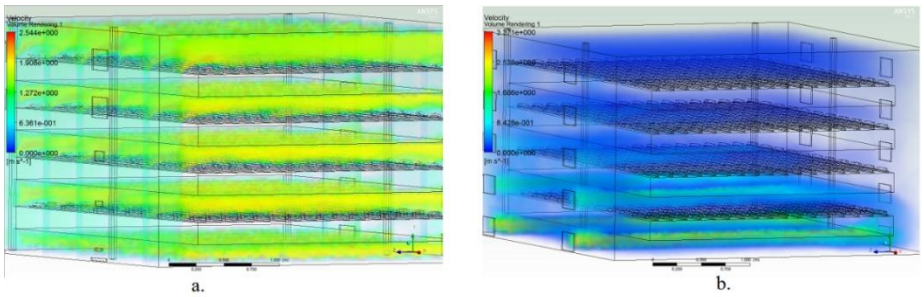

Fig. 11. Lateral view of the prover and air speed distribution at: a) different discharge grids, fan at 50 HZ; b) equal discharge grids, fan at 50 Hz

It can be seen a much better air speed uniformity throughout the entire prover. Higher speeds are still registered at C, D and E grids but the maximum reached speed is 2.1 m/s and the maximum speed which passes over the dough pieces is 0.8 m/s. This air speed does not affect the proving process in any way.

For further verifications, simulations were run at different air flows, starting from 1650 m³/h (at 20 Hz fan frequency) to 2200 m³/h (50 Hz fan frequency) at 10 Hz interval. The results are presented in figure 12.

In all 4 simulations, it was observed a gradual increase of the points in which the air speed reaches 0.6 m/s. The best results were obtained when the fan works at 50 Hz and the measured air flow is 2200 m³/h.

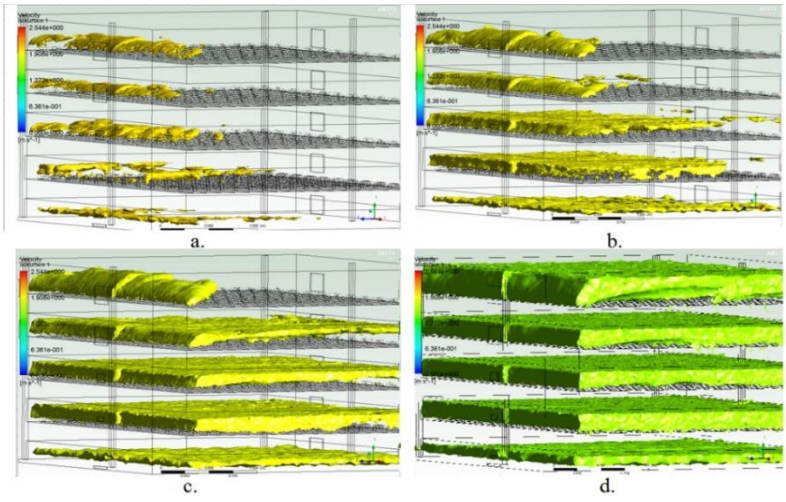

Fig. 12. Air speed distribution in all points where it reaches 0.6 m/s: a) simulation with fan functioning at 20 Hz; b) simulation with fan functioning at 30 Hz; c) simulation with fan functioning at 40 Hz; d) simulation with fan functioning at 50 Hz

For simulation accuracy, real measurements for air speed distribution were taken in the prover, during full cycle working of 60 minutes, in both presented cases. The measurements were taken in three points on each floor, at grid discharge, floor entrance and exit, respectively. Each measurement was taken at 5 minute interval. The mean values are presented in table 2 and the resulting graphics in figures 13 and 14.

Table 2

Means of measured values in three points on each floor of the prover

Grid	Equal grids	Floor entrance	Floor exit	Different grids	Floor entrance	Floor exit
Frequency [50 Hz]						
Air speed values [m/s]						
A	0.32	0.12	0.05	0.35	0.31	0.58
B	0.51	0.21	0.09	0.63	0.48	0.61
C	0.88	0.30	0.10	0.81	0.62	0.65
D	1.43	0.42	0.31	1.35	0.73	0.69
E	3.23	0.52	0.40	2.21	1.00	0.72

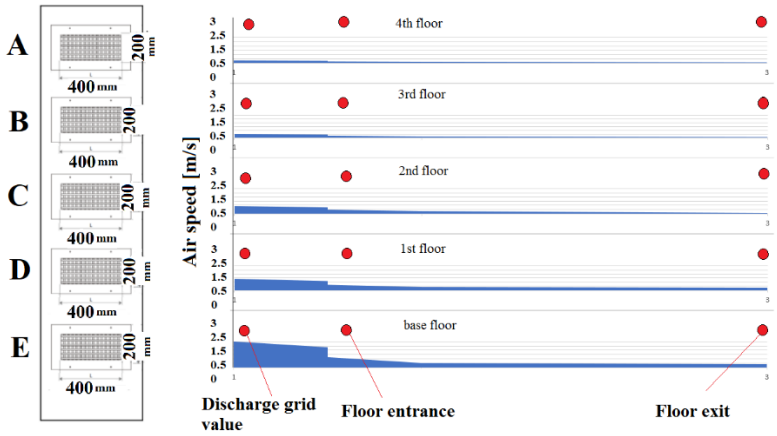

Fig. 13. Graphic representation of measured air speed values on each floor of the prover, using equal grid dimensions

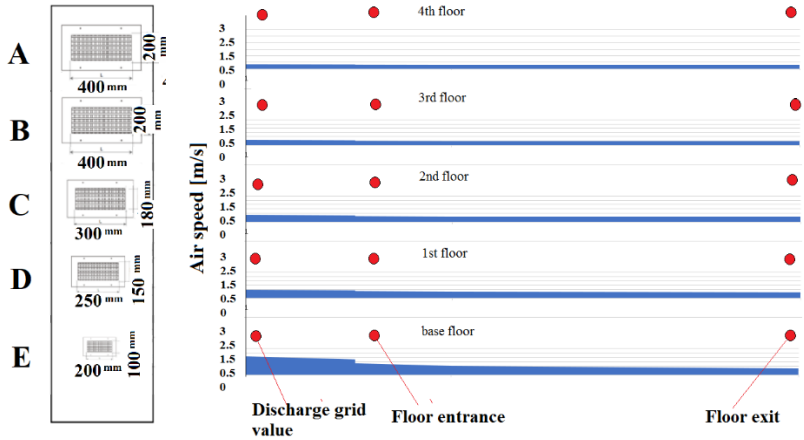

Fig. 14. Graphic representation of measured air speed values on each floor of the prover, using different grid dimensions

In figures 13 and 14, the highlighted points represent the places where the measurements were taken: at the grid level, floor entrance and floor exit (from left to right).

Although the tridimensional simulation could not generate actual values on different selected points of the designed prover, the simulation's accuracy can be confirmed in a high percentage by comparing the results of the simulation presented in figure 10 with the results obtained by measuring the air speed in the real prover and presented in figures 13 and 14.

4. Conclusions

The first simulations showed a direct connection between the air speed and the temperature distribution in the prover. The more uniformly distributed the air speed in the prover, the more stable the temperature gradient throughout the prover is, at least in static considered environment. The optimal air speed for dough proving was determined at 0.6 m/s, a value which travels the entire distance between discharge and charge system and does not affect the product quality, as was later verified experimentally.

The results obtained when the fan frequency was increased (the air speed) were not satisfying. The best results were obtained by modifying the air discharge grids on the first three levels of the prover (C, D, E) to dimensions which, next to an air speed of 0.6 m/s, it uniformly distributes the temperature to all the 4 floors of the prover.

Better results can be obtained by modifying the grids dimensions to counter the pressure loss and determine the appropriate air speed at the discharge grids, in concordance with the air speed distribution in the entire volume of the prover. The optimal air flow pattern determination can lead to a more accurate control of the proving working regime, resulting in finished products with constant quality regarding volume, texture and overall fermentation characteristics.

The numerical simulation program can be used for designing more efficient air conditioning systems for dough proving and highlights the necessity for taking into consideration all the technical and technological aspects of dough proving.

R E F E R E N C E S

[1] *A. Istudor, Gh. Voicu, Gh. Muscalu, M. Munteanu*, Final bread dough fermentation – requirements, conditions, equipment. A short review, INMA-TEH, 2017, pp.519-526;

[2] *P. Shah, G. M. Campbell, S. L. McKee & C. D. Rielly*, Proving of bread dough: modelling the growth of individual bubbles. Transactions of the Institution of Chemical Engineers, Part C, **Vol 76**, 1998, pp. 73–79;

[3] *Gheorghe Voicu*, Procese şi utilaje pentru panificaţie (Processes and equipment for bread making), Editura Bren, Bucureşti, 1999;

[4] *Burgess Hill Jennings*, The Thermal Environment: Conditioning and Control. Harper & Row, New York, 1978;

[5] *Emil Alexandru Brujan*, Ventilația și condiționarea aerului (Air conditioning and ventilation), Editura Printech, București, 2004;
[6] *Gh. Duță, N. Niculescu, P. Stoenescu,* Instalații de ventilare și climatizare (Acclimation and ventilation installations), editura Artenco București, 2002;
[7] *M. Nagi, O. Bancea, S. Dorhoi*, Ventilarea si climatizarea cladirilor, Colectia student, (Ventilation and acclimation of buildings, Student collection), Editura Politehnica Timisoara, 2007;
[8] *C. Miron, L. Miron, I. Puscasu, M. Chereches*, Ghid de buna practica pentru proiectarea instalatiilor de ventilare si conditionare in cladiri, (Good practices guide for conditioning and ventilation installations in buldings), INCD URBAN –INCERC, mai, 2012;
[9] *D. Etheridge, M. Sandberg*, Building ventilation — theory and measurement. Chichester, UK: John Wiley & Sons, 1996;
[10] *Peter Nielsen*, Flow in air conditioned rooms, PhD Thesis, Technical University of Denmark, Copenhagen, 1974;
[11] *H.B. Awbi*, Application of computational fluid dynamics in room ventilation, Building and Environment (24)1, 1989, pp. 73-84;
[12] *A.J. Baker, P.E. Williams, P.E. Kelso*, Numerical calculation of room air motion – part 1: math, physics and CFD modeling, ASHRAE Transactions 100(1), 1994, pp. 515-530;
[13] *G. Gan, H.B. Awbi*, Numerical simulation of the indoor environment. Building and Environment 29(4), 1994, pp: 449-459;
[14] *P. Nielsen*, Prediction of airflow and comfort in air conditioned spaces. ASHRAE Transactions 81, 1975, pp. 247-259;
[15] *Z. Weibiao, T. Nantawan*, Three dimensional CFD Modeling of Continuous Industrial Baking Process, in Computational Fluid Dynamics in Food Processing, Second edition, CRC press, 2019, pp. 193
[16] *J. Aubin, C. Xuereb*, Design of Multiple Impeller Stirred Tanks for the mixing of highly viscous fluids using CFD. Chem Eng Sci 61, 2006, pp. 2913-2920;
[17] *R. K. Connely*, Computational fluid dynamics simulation of dough mixers, Cereal Foods world, **vol. 53**, nr.4, 2008, pg. 198-204;
[18] *Gh. Muscalu, Gh. Voicu, A. Istudor, P. Tudor*, Bread dough rheological behaviour under the influence of the geometry of the kneading arms, Revista de Chimie, **vol. 71** (9), 2020, pp. 295-307;
[19] *U. De Vries, H. Velthuis, K. Koster*, Baking ovens and product quality- a computer model. Food Sci Tech Today 9, 1995, pp. 232-234;
[20] *N. Therdthai, W. Zhou, T. Adamczak*, Two-dimensional CFD modelling and simulation of industrial continuous bread baking oven. J Food Eng. (60), 2003, pp. 211-217;
[21] *M. Boulet, B. Marcos, M. Dostie, C. Moresoli*, CFD modeling of heat transfer and flow field in a bakery pilot oven. Journal of Food Engineering, **vol 97**(3), 2010, pp. 393–402;
[22] *Charlotte Atchley*, Promoting airflow in proofers, Article in Baking Business online magazine, march, 2016, https://www.bakingbusiness.com/articles/39664-promoting-airflow-in-proofers accesat la data de 03.02.2021;
[23] *Charles Hirsch*, Numerical computation of internal and external flows, **Vol. 2,** Computational methods for inviscid and viscous flows, 1990, pp: 604-606;
[24] Fluent Guide-Multiphase Flow Regimes, in Ansys fluent 12.1, 2009;
[25] *C. R. Swaminathan, V. R. Voller,* A General Enthalpy Method for Modeling Solidification Processes. Metallurgical Transactions B, 23B ,1992, pp. 651-664;
[26] *V. Voller, C. Prakash,* A Fixed-Grid Numerical Modeling Methodology for Convection-Diffusion Mushy Region Phase-Change Problems. Int. J. Heat Mass Transfer, **vol.30**, 1987, pp. 1709-1720;
[27] *V. R .Voller, C. R. Swaminathan*, Generalized Source-Based Method for Solidification Phase Change. Numer. Heat Transfer B, **vol. 19**, 1991, pp. 175-189;
[28] *A. K. Nayak, P. P. Kulkarni, P. Pandey, S. V. Prasad,* Modelling of core melt scenarios in nuclear reactors in Advances of Computational Fluid Dynamics in Nuclear Reactor Design and Safety Assessment, 2019.